Science Advances
AAAS

advances.sciencemag.org/cgi/content/full/6/32/eaba8415/DC1

Supplementary Materials for

Daxx maintains endogenous retroviral silencing and restricts cellular plasticity in vivo

Amanda R. Wasylishen*, Chang Sun, Sydney M. Moyer, Yuan Qi, Gilda P. Chau, Neeraj K. Aryal, Florencia McAllister, Michael P. Kim, Michelle C. Barton, Jeannelyn S. Estrella, Xiaoping Su, Guillermina Lozano*

*Corresponding author. Email: awasylishen@mdanderson.org (A.R.W.); gglozano@mdanderson.org (G.L.)

Published 5 August 2020, *Sci. Adv.* **6**, eaba8415 (2020)
DOI: 10.1126/sciadv.aba8415

The PDF file includes:

Other Supplementary Material for this manuscript includes the following:

(available at advances.sciencemag.org/cgi/content/full/6/32/eaba8415/DC1)

Fig. S1

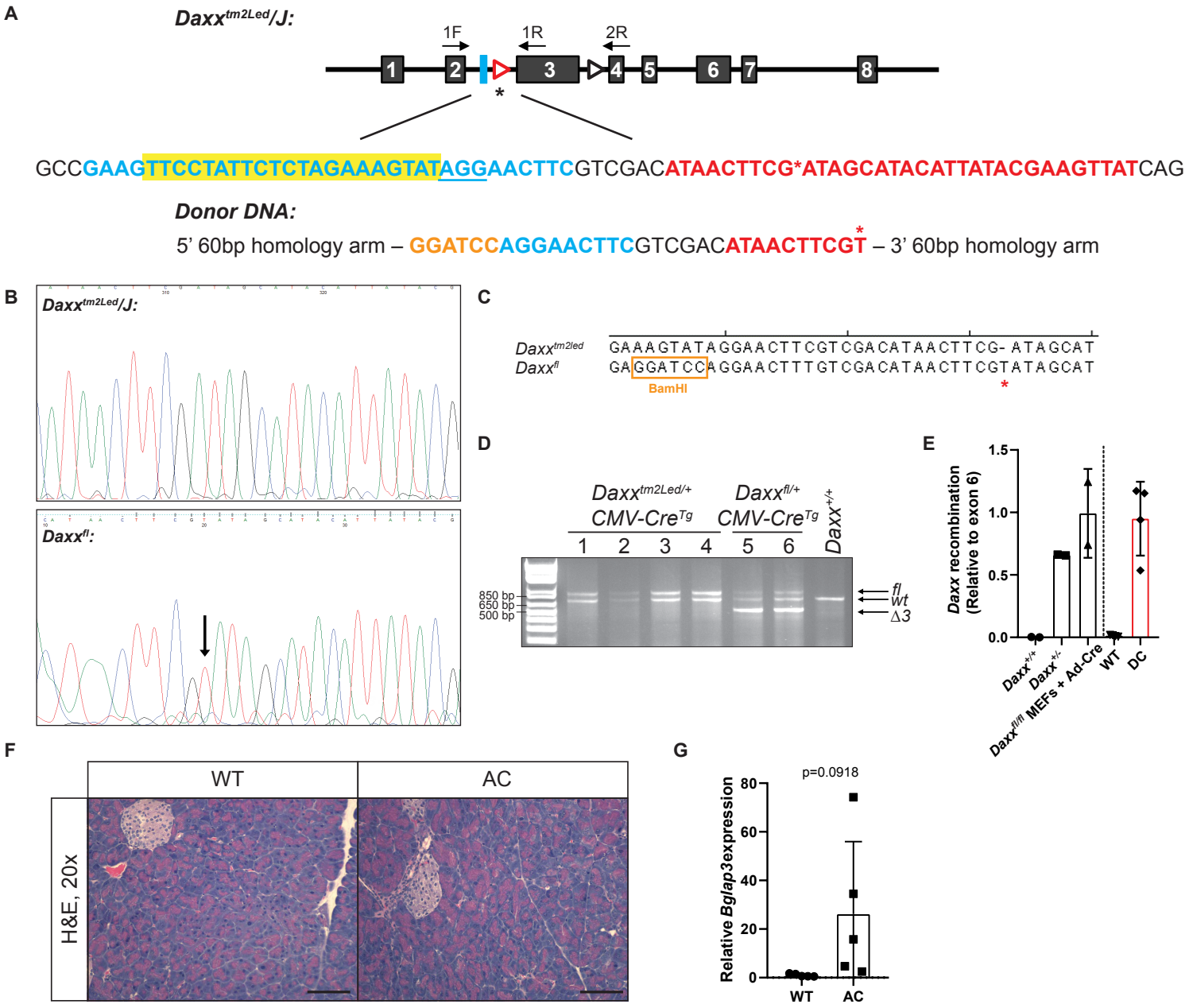

Fig. S1: *Daxx* or *Atrx* loss in the developing mouse pancreas

(A) Schematic representation of the *Daxx*^{tm2Led} allele with the gene targeting strategy depicted. The remaining FRT sequence is indicated in blue, and the loxP sites are indicated by triangles, with the non-functional loxP sequence in red. The n20 sequence is highlighted in yellow, with the protospacer adjacent motif underlined. The location of the single nucleotide deletion is indicated with an asterisk. The provided donor DNA sequence includes a BamHI site (orange), and the fixed loxP sequence. Genotyping primers are indicated by arrows. (B) Chromatogram depicting successful homologous recombination and generation of the *Daxx*^{fl} allele. (C) Sequence alignment of *Daxx*^{tm2Led} and *Daxx*^{fl} alleles. (D) PCR genotyping comparing recombination induced by the *CMV-Cre*^{Tg} mouse. WT, wild-type. (E) Quantitative PCR assay evaluating recombination in the pancreas of *Daxx*$^{fl/fl}$*Pdx1-Cre*^{Tg} (DC) mice. Primers are designed to recognize the recombined allele, and data are normalized to exon 6. Controls for recombination include tail biopsies from *Daxx*$^{+/-}$ mice and *Daxx*$^{fl/fl}$ mouse embryo fibroblasts (MEFs) that have been treated with adenoviral Cre (Ad-Cre) and have no detectable Daxx protein according to Western blot analysis (data not shown). (F) Representative hematoxylin and eosin (H&E)-stained sections of 6 week old WT and *Atrx*$^{fl/fl}$*Pdx1-Cre*^{Tg} (AC) mouse pancreases. Image magnification is 20x, scale bar = 100 μm. (G) Quantitative reverse-transcription PCR for *Bglap3* expression, shown as mean ± standard deviation. p = 0.0918, Student *t*-test.

Fig. S2

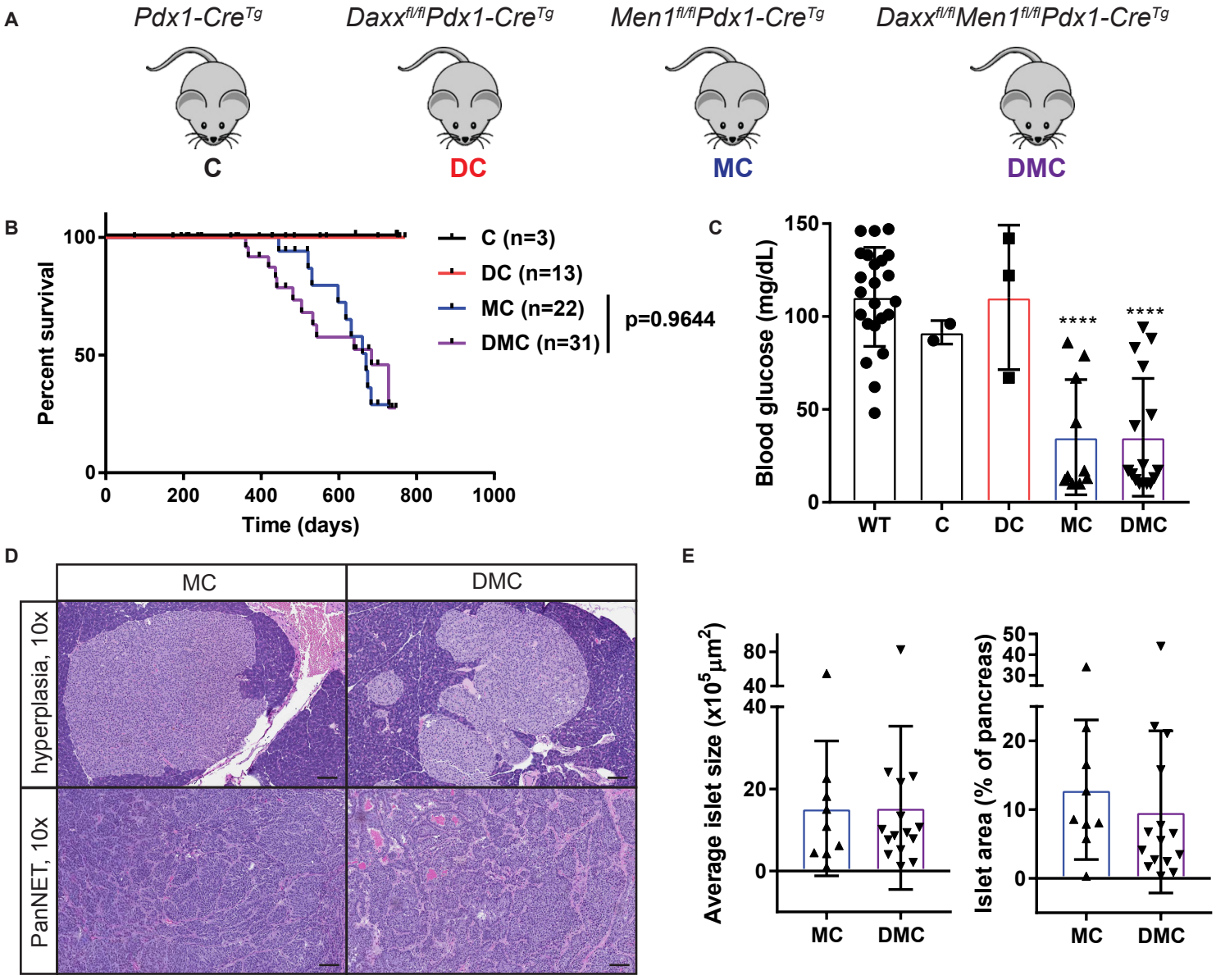

Fig. S2: *Daxx* loss does not cooperate with *Men1*-deficiency to promote endocrine tumorigenesis in mice
(A) Schematic representation and short form notation of mice in cohort. C, *Pdx1-Cre*^{Tg}; DC, *Daxx*$^{fl/fl}$*Pdx1-Cre*^{Tg}; MC, *Men1*$^{fl/fl}$*Pdx1-Cre*^{Tg}; DMC, *Daxx*$^{fl/fl}$*Men1*$^{fl/fl}$*Pdx1-Cre*^{Tg}. (B) Kaplan-Meier survival analysis. The C and DC mice are the same as those presented in Figure 1D. (C) Non-fasting blood glucose analysis of mice at necropsy (mean ± standard deviation). ****, $p < 0.0001$, analysis of variance with Dunnett multiple comparisons test relative to wild-type (WT) mice. (D) Representative hematoxylin and eosin-stained images of hyperplasias and pancreatic neuroendocrine tumors observed in MC and DMC mice. Image magnification is 10x, scale bar = 100 µm. (E) Quantification of the endocrine pancreas compartment in DMC compared to MC mice (mean ± standard deviation).

Fig. S3

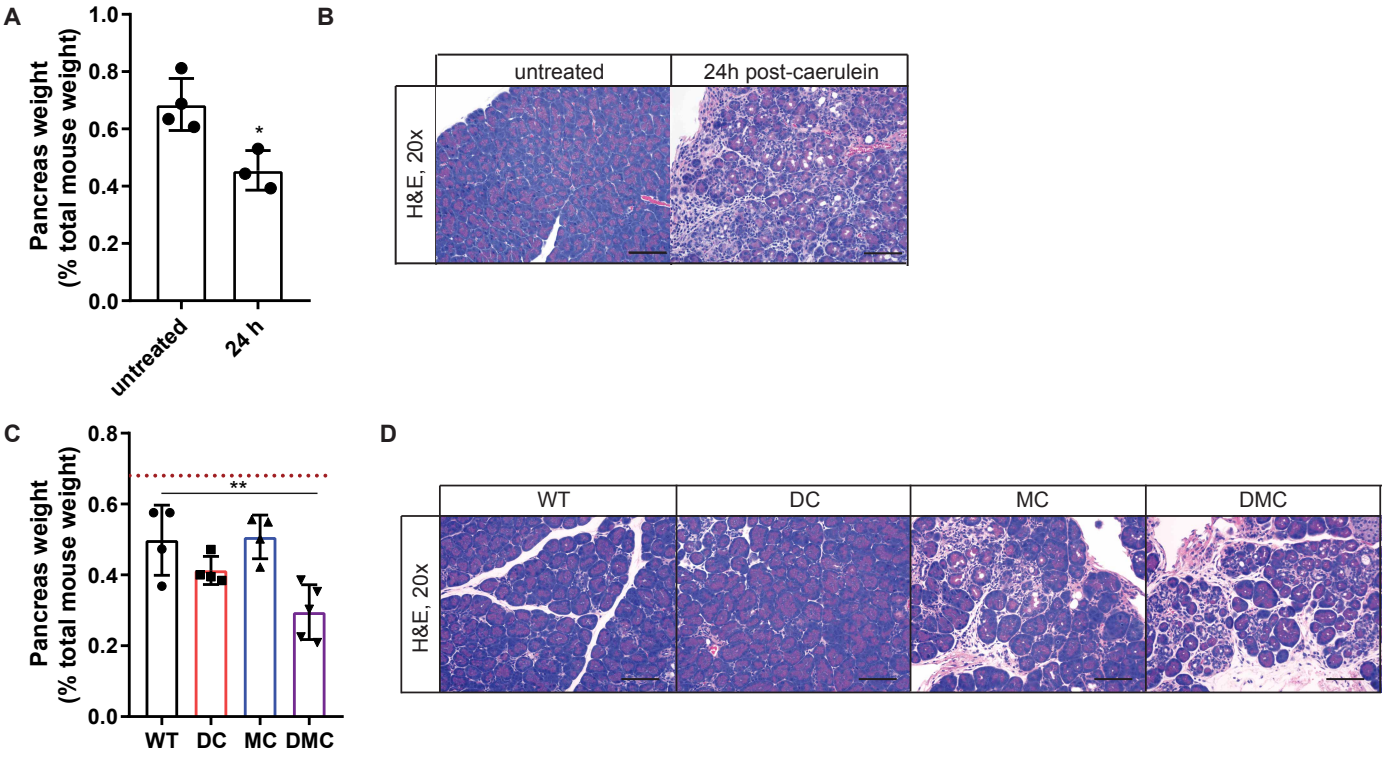

Fig. S3: Response to chronic pancreatitis
(A) Pancreas weight of wild-type (WT) mice 24 hours following treatment with caerulein or no treatment (mean ± standard deviation). *p<0.05, Student *t*-test. (B) Representative hematoxylin and eosin (H&E)-stained images of wildtype mouse pancreas sections 24 hours following the final dose of caerulein or no treatment. Image magnification is 20x, scale bar = 100 μm. (C) Pancreas weight 5 days following the final dose of caerulein (mean ± standard deviation). The dotted line represents the average weight of an untreated WT pancreas. **p<0.01, analysis of variance with Dunnett post-test relative to caerulein-treated WT. DC, *Daxx*$^{fl/fl}$*Pdx1-Cre*^{Tg}; MC, *Men1*$^{fl/fl}$*Pdx1-Cre*^{Tg}; DMC, *Daxx*$^{fl/fl}$*Men1*$^{fl/fl}$*Pdx1-Cre*^{Tg}. (D) Representative H&E-stained images 5 days following the final dose of caerulein. Images magnification is 20x, scale bar = 100 μm.

Fig. S4

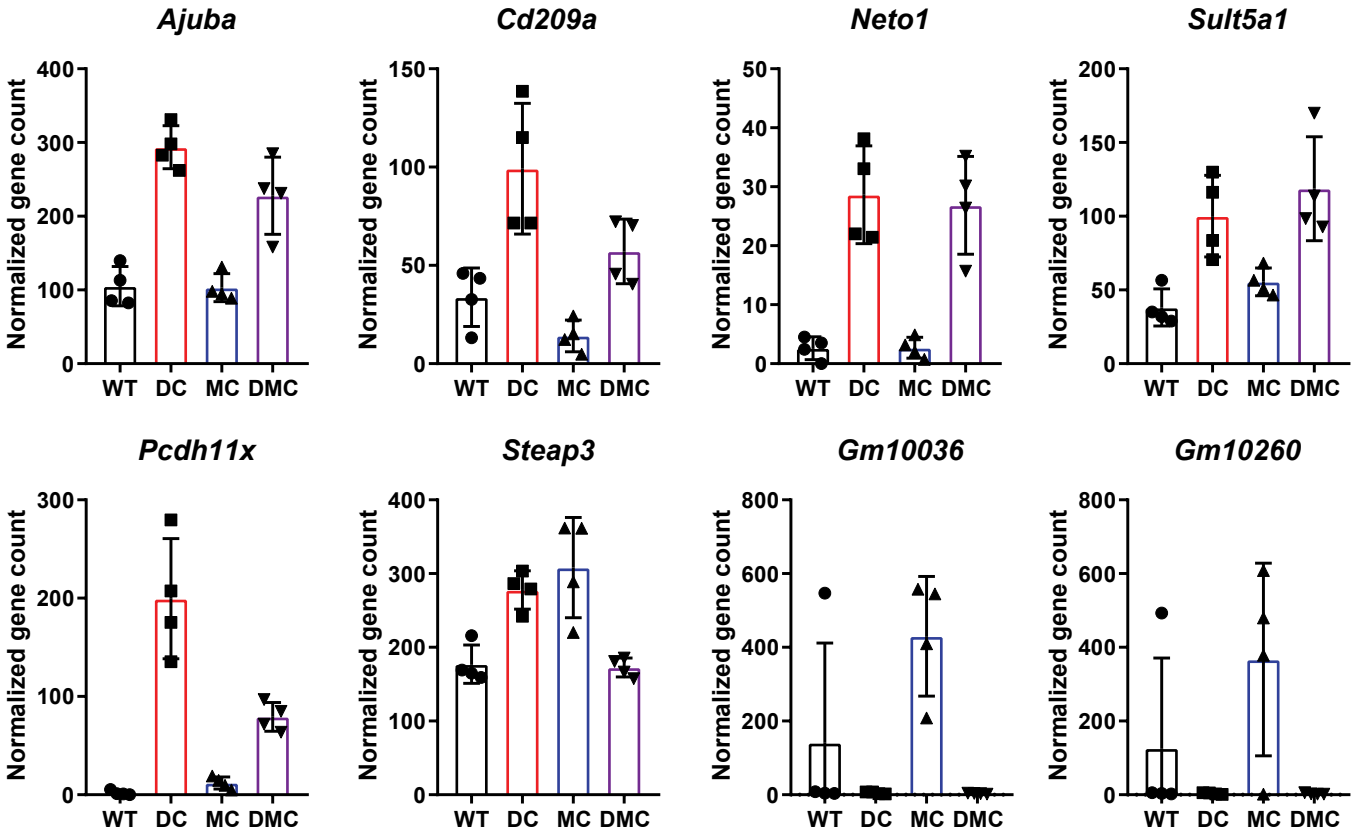

Fig S4: Daxx-dependent gene expression changes from RNA sequencing data
Base means from RNA sequencing data of common genes from comparison between genotypes (mean ± standard deviation). WT, wild-type; DC, *Daxx*$^{fl/fl}$*Pdx1-Cre*^{Tg}; MC, *Men1*$^{fl/fl}$*Pdx1-Cre*^{Tg}; DMC, *Daxx*$^{fl/fl}$*Men1*$^{fl/fl}$*Pdx1-Cre*^{Tg}.

Table S2: Significant Daxx-dependent gene expression changes in genes that define pancreas cell types

		DC vs WT	
Cell type	Gene	Log_2FC	P_{adj}
Epsilon[1]	*Sptssb*	4.04	4.90×10^{-2}
	*Prox1**	0.65	4.11×10^{-2}
Duct[1]	*Mmp7*	1.82	1.69×10^{-2}
	*Onecut2**	2.24	1.38×10^{-2}
Mesenchyme[1]	*Col1a1*	1.11	1.96×10^{-2}
	Col1a2	0.91	1.61×10^{-2}
	Col3a1	0.89	1.71×10^{-2}
	Col5a1	0.89	2.90×10^{-3}
	*Fbn1**	0.76	2.59×10^{-2}
	*Prrx1**	1.25	1.39×10^{-3}
Alpha[1]	*Plce1*	0.97	1.12×10^{-2}
	Gc	1.09	2.42×10^{-2}
Delta[1]	*Hhex**	0.73	1.93×10^{-2}
Stellate[2]	*Mmp2*	0.98	2.91×10^{-3}
	Fgf2	0.94	1.73×10^{-2}
	Col1a1	1.11	1.96×10^{-2}
	Pdgfra	0.68	4.31×10^{-2}
Standard	*Col1a1*	1.10	1.96×10^{-2}
Activated stellate[2]	*Timp3*	0.85	2.66×10^{-2}
	Col6a1	0.75	4.76×10^{-2}
	Col1a2	0.91	1.60×10^{-2}
	Col3a1	0.89	1.71×10^{-2}
	Ctgf	1.44	3.49×10^{-3}

*=transcription factor

References: [1]Muraro et al., 2016, Cell Systems 3, 385–394; [2]Baron et al., 2017, Cell Systems 3(4), 346-360.

DC, *Daxx*$^{fl/fl}$*Pdx1-Cre*^{Tg}; WT, wild-type.